Correspondence to:
T. Pitkänen,
timo.pitkanen@space.umu.se

Relevance of the North-South Electric Field Component in the Propagation of Fast Convective Earthward Flows in the Magnetotail: An Event Study

T. Pitkänen[1,2] [ID]**, M. Hamrin[1]** [ID]**, G. S. Chong[1]** [ID]**, and A. Kullen[3]** [ID]

[1]Department of Physics, Umeå University, Umeå, Sweden, [2]Space Physics and Astronomy Research Unit, University of Oulu, Oulu, Finland, [3]Department of Space and Plasma Physics, School of Electrical Engineering and Computer Science, Royal Institute of Technology, Stockholm, Sweden

Abstract Fast earthward plasma flows are commonly observed in the magnetotail plasma sheet. These flows are often termed as bursty bulk flows because of their bursty nature, and they are considered to be generated by magnetic reconnection. Close to the neutral sheet ($B_x \sim 0$), the fast flows are considered to be associated with an enhanced dawn-to-dusk electric field ($E_y > 0$), which together with the northward magnetic field component ($B_z > 0$) protrude the plasma earthward via enhanced $E \times B$-drift. Sometimes, reversals in the dawn-dusk velocity component perpendicular to the magnetic field ($V_{\perp y}$) are measured in association with B_x sign changes in the flows. This suggests that the electric field component in the north-south direction (E_z) can play a role in determining the dawn-dusk direction of the enhanced drift. We present data measured by the Magnetospheric Multiscale, which demonstrate that E_z can have a dictating role for $V_{\perp y}$ of fast flows. Furthermore, it is shown that the critical contribution of E_z is not limited only to $V_{\perp y}$, but it can also dominantly determine the enhanced drift of the fast flows in the X direction ($V_{\perp x}$). The latter can occur also near and at the neutral sheet, which adds an alternative configuration to the conventional picture of E_y and B_z being the main players in driving the earthward fast flows. The domination of E_z in the studied events appears with potential signatures of an influence of a nonzero dawn-dusk component of the interplanetary magnetic field (IMF B_y) on the magnetotail.

1. Introduction

The magnetotail plasma sheet is commonly accommodated by intermittent earthward high-speed ion bulk flows, often termed as fast flows, flow bursts, or bursty bulk flows (BBFs) (Angelopoulos et al., 1992, 1994; Baumjohann et al., 1990; Cao et al., 2006; Raj et al., 2002). These longitudinally localized high-speed flows with speeds ranging from ∼100 to ∼1,000 km/s are considered to be generated by magnetic reconnection. They are observed to occur in bursts with a typical duration ranging from 10 s to 1 min. Many individual bursts can appear in a sequence forming a BBF event of a typical time scale of 10 min.

Theoretically, a fast flow represents depleted magnetic flux tubes that are polarized on the flanks in the equatorial plane due to reduced cross-tail current inside the tubes (Chen & Wolf, 1993). The dawn-to-dusk polarization electric field (E_y) and northward magnetic field (B_z) drive fast plasma and magnetic flux earthward by enhanced $E \times B$-drift. E_y gives directly an estimate for the earthward magnetic flux transport per unit length along the Y axis.

Thus, it is of no surprise that E_y has been the most studied electric field component in BBF and studies (e.g., Angelopoulos et al., 1992, 1994; Kauristie et al., 2000; Nakamura, Baumjohann, Brittnacher, et al., 2001; Nakamura, Baumjohann, Schödel, et al., 2001; Sergeev et al., 2000; Shue et al., 2008). Schödel, Baumjohann, et al. (2001) and Schödel, Nakamura, et al. (2001) have included an estimate of the E_x component (aligned along the Sun-Earth line) and studied BBFs by defining "rapid flux transport" events by an estimate for the electric field in the XY plane, $E_H = \sqrt{\left(\left(V_x B_z\right)^2 + \left(V_y B_z\right)^2\right)} > 2$ mV/m when $V_\perp > V_\parallel$.

An oppositely directed dawn-dusk ion velocity component perpendicular to the magnetic field ($V_{\perp y}$) has been measured above and below the neutral sheet in a BBF event (Grocott et al., 2007). Furthermore, $V_{\perp y}$ has been observed to reverse in association with a B_x sign change (Pitkänen et al., 2015; Walsh et al., 2009). Solar wind and conjugate observations of ionospheric convection in these events suggest a connection to
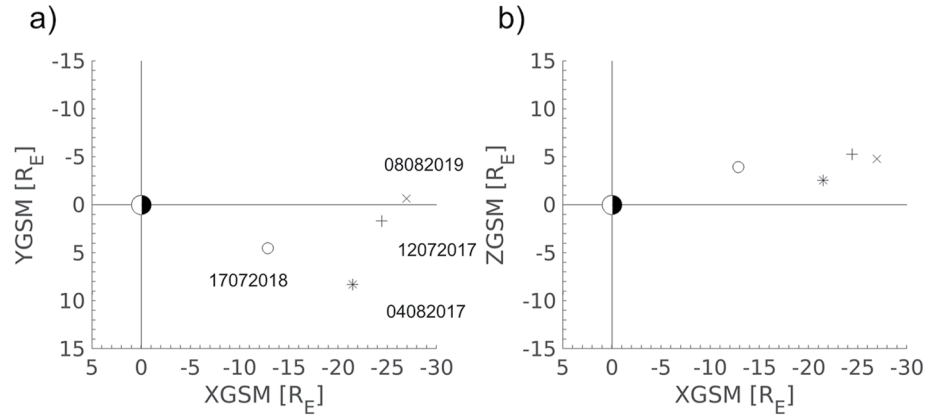
Figure 1. Locations of the measured fast flow events in the (a) geocentric solar magnetospheric (GSM) *XY* plane and (b) GSM *XZ* plane. The dates of the events are marked.

the direction of the dawn-dusk component of the interplanetary magnetic field (IMF B_y). The interhemispheric asymmetry in $V_{\perp y}$ in the midnight sector found in the statistical studies of fast flows (Pitkänen et al., 2013, 2017) and slow flows (Pitkänen et al., 2019) support the interpretation that IMF B_y has an influence on magnetotail convection.

One can assume that the frozen-in condition generally holds outside the reconnection regions in the magnetotail. Under such conditions, the measured ion velocity perpendicular to the magnetic field is mostly determined by the $E \times B$ velocity:

$$\mathbf{V}_\perp = \frac{1}{B^2}\Big[\big(E_y B_z - E_z B_y\big)\mathbf{u}_x + \big(E_z B_x - E_x B_z\big)\mathbf{u}_y + \big(E_x B_y - E_y B_x\big)\mathbf{u}_z\Big], \tag{1}$$

where $\mathbf{u}_x$, $\mathbf{u}_y$, and $\mathbf{u}_z$ are the unit vectors. We note that not only E_x and E_y contribute to $V_{\perp x}$ and $V_{\perp y}$, but also E_z plays a role. The results discussed above, of $V_{\perp y}$ reversals as B_x changes its sign, suggest that E_z can be important in the determination of $V_{\perp y}$. Also, in certain conditions, the $-E_z B_y$-term could dominate in $V_{\perp x}$.

In this study, we investigate the ion drift in fast flow events measured by the Magnetosphere Multiscale (MMS) mission showing clear $V_{\perp y}$ reversals, and the relative importance of different $E_i B_j$-terms (where i and j go through x, y, and z) in determining $V_{\perp x}$ and $V_{\perp y}$ according to Equation 1. The paper is organized as follows: In Section 2, the data are described and the flow events are analyzed. In Section 3, we discuss the results and in Section 4, we present a short summary.

2. Observations

2.1. Flow Events and Data

In this study, we investigate four fast flow events that were measured in the magnetotail by MMS. The locations of the events in the geocentric solar magnetospheric (GSM) *XY* and *XZ* planes with the date information are displayed in Figure 1.

We present data only from the MMS 1 spacecraft, because the measurements from all the satellites are very similar due to close interspacing of the spacecraft (between 11 and 75 km). The magnetic field measurements are from the fluxgate magnetometers (digital fluxgate DFG and analog fluxgate AFG) (Russell et al., 2016) in the FIELDS instrument suite (Torbert et al., 2016). The sampling frequency of the magnetic field data is 16 Hz. The particle data are ion data from the Fast Plasma Investigation (FPI) (Pollock et al., 2016). The FPI instrument measures ions with energies over the range from 10 eV/q to 30 keV/q, where q is the charge of the particle. While FPI acquires the full 3-D ion distribution in 150 ms in the burst mode, we use the FPI survey mode data with a 4.5-s time resolution. The electric field data are measured by the electric field instruments (Spin-plane Double Probe SDP and Axial Double Probe ADP) in the FIELDS
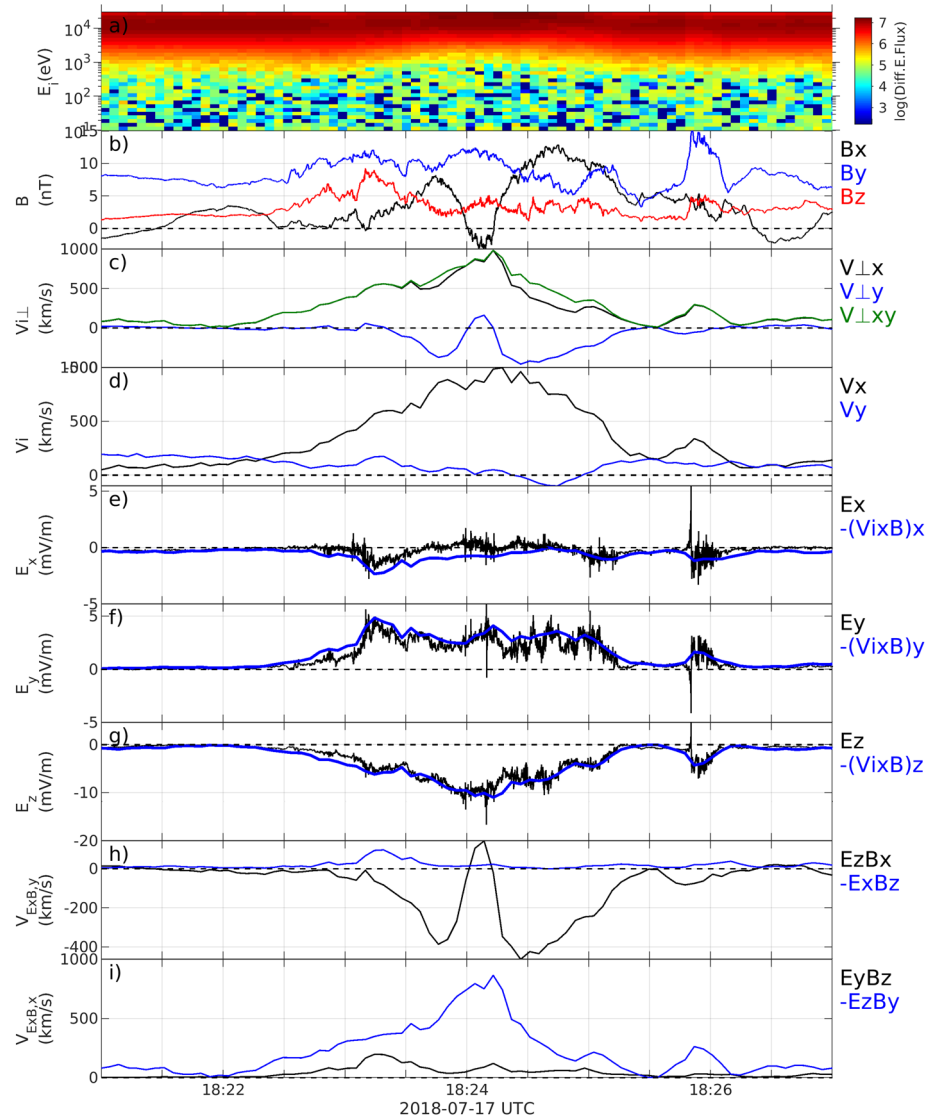
Figure 2. Magnetospheric Multiscale 1 data for flow event 1. (a) Omnidirectional energy-time spectrogram of the differential energy flux for ions. (b) Magnetic field. (c) Ion velocity perpendicular to the magnetic field. The green curve marks $V_{\perp xy} = \sqrt{V_{\perp x}^2 + V_{\perp y}^2}$. (d) Ion total velocity. (e–g) Electric field components from the direct measurements by FIELDS (black) and computed from the ion velocity and the magnetic field (blue). (h) The two terms of the Y component of the $E \times B$ velocity. (i) The two terms of the X component of the $E \times B$ velocity. The division by B^2 has been left out when writing the different terms in the right hand side of panels (h and i).

suite (Ergun et al., 2016; Lindqvist et al., 2016) with a sampling frequency of 32 Hz. In addition, we discuss IMF data, which are from the OMNI database (propagated to the nominal bow shock nose) (https://omni-web.gsfc.nasa.gov/) (King & Papitashvili, 2005) and SuperMAG auroral electrojet (SME) index data (https://supermag.jhuapl.edu) (Gjerloev, 2012; Newell & Gjerloev, 2011). The time resolution of both the IMF and SME index data is 1 min. All the satellite data are presented in the GSM coordinate system throughout the paper.

2.2. Flow Event 1: July 17, 2018

Figure 2 displays MMS 1 data for fast flow event 1, which was detected at ∼18:24 UTC on July 17, 2018. The event appeared in the premidnight sector at $[-12.8, 4.5, 4.0]$ R_E (R_E = earth radius) (Figure 1). The omnidirectional differential energy flux data in Figure 2a indicate that MMS 1 measured >keV ions in the plasma
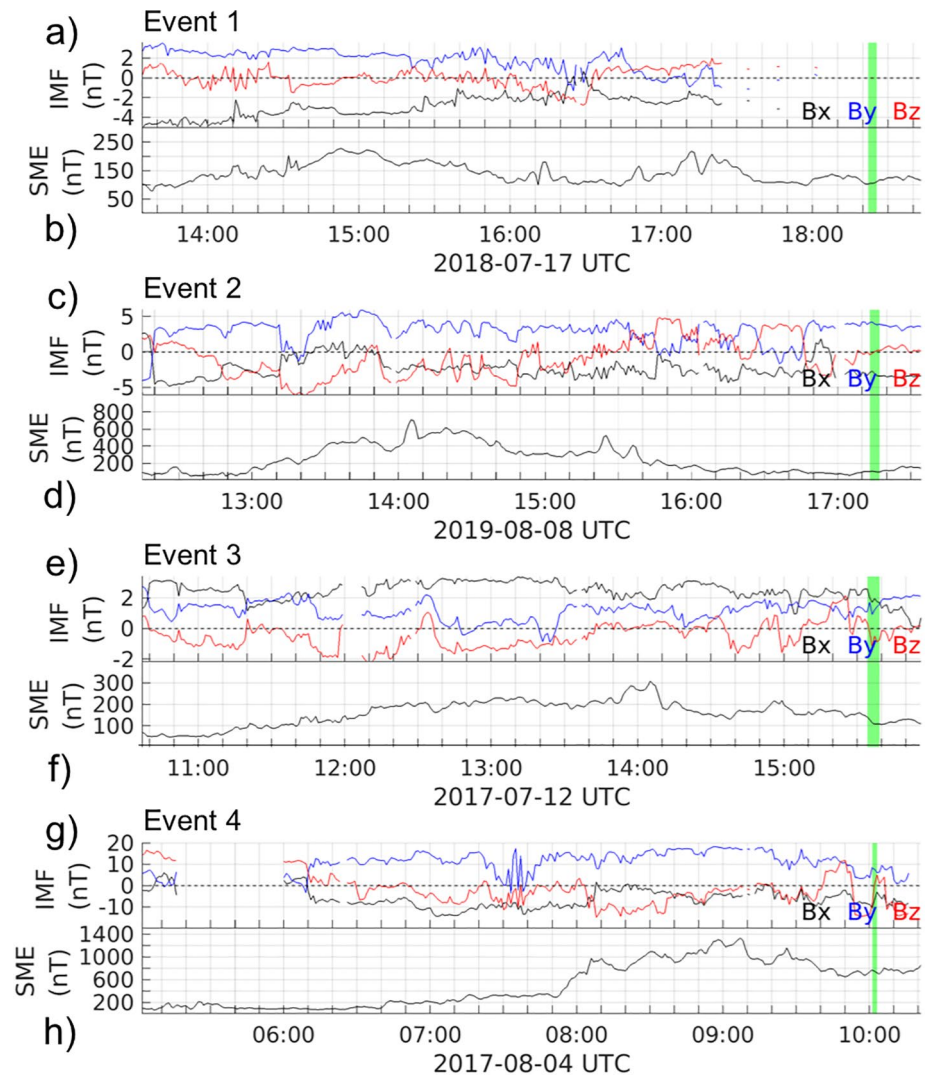
Figure 3. (a, c, e and g) The interplanetary magnetic field (IMF) and (b, d, f and h) The SuperMAG auroral electrojet (SME) index during a time interval between 5 h prior to and 20 min after each fast flow event. The times of the flow events are marked by green shading.

sheet. During the event, the lower boundary of the intense energy flux appeared to increase slightly from 1 to 3 keV between 18:23:05 and 18:25:07 UTC.

The earthward velocity X component in the event peaks at 1,000 km/s for both the X components of the total velocity V_x (Figure 2d) and the velocity perpendicular to the magnetic field $V_{\perp x}$ (Figure 2c), which is a considerable value at this close distance from Earth. From the magnetic field measurements, we see that both B_y and B_z were rather stable and clearly positive during the event (Figure 2b). A smaller and larger dipolarization front in B_z can be noticed at ~18:22:50 UTC and ~18:23:10 UTC, respectively. B_x is mostly positive, and associated positive B_y is to an opposite direction that what is expected from the azimuthal field line flaring in the premidnight sector. The latter could be interpreted as a signature of a twisting of closed field lines due to the positive IMF B_y influence. While the IMF data are sparse after 17:24 UTC, we can say that IMF B_y was varying between positive and negative values during the preceding 1.5 h and it was slightly positive (between 1 and 3 nT) before that for several hours (Figure 3a). Because there appears positive tail B_y in the unexpected direction (comparing the field caused by the flaring), there is a possibility that this was induced by IMF B_y (field line twisting), as IMF B_y was predominantly positive during several hours before the flow event. However, we cannot be sure due to the lack of the IMF data during the last 1.5 h before the

event, and potential other sources contributing to tail B_y (see discussion in Section 3). The SME index data indicate that the fast flow event was measured after intensifications of the electrojets in the ionosphere at around 15 UTC and after 17 UTC with maximum SME of 229 and 220 nT, respectively (Figure 3b). This suggests that the flow event occurred in the recovery phase of weak substorm activity.

In the middle of the fast flow, B_x made an excursion to negative at 18:24 UTC (Figure 2b). This was accompanied by a duskward excursion of otherwise mainly dawnward $V_{\perp y}$ (Figure 2c). The excursions lasted ∼13 s. A comparison of the $-\mathbf{V} \times \mathbf{B}$ electric field components (blue curves in Figures 2e–2g) to the corresponding direct electric field measurements (black curves in Figures 2e–2g), shows matching and indicates that the frozen-in condition was satisfied. The electric field components E_y and E_z are clearly positive and negative, respectively, over the entire BBF event.

To investigate the relative importance of the different electric and magnetic field components in the perpendicular velocity, we have plotted the two $E_i B_j$-terms (where i and j go through x, y, and z) for the Y and X components of the $E \times B$ velocity given in Equation 1, in Figures 2h and 2i. The used electric field is the $-\mathbf{V} \times \mathbf{B}$ electric field. In Figure 2h, we note that the $E_z B_x$-term dominates $V_{\perp y}$: E_z stays negative with a quite large magnitude (Figure 2g) and B_x has the excursion to negative (Figure 2b). The $-E_x B_z$-term instead, is small throughout the event and has no role in the $V_{\perp y}$ variations. Thus, E_z is the relevant electric field component, not E_x, in the determination of the dawn-dusk perpendicular velocity direction. In Figure 2i, we also see that the $-E_z B_y$-term is clearly dominant over the $E_y B_z$-term in the $V_{\perp x}$. Thus, again E_z is the relevant electric field component. This yields also in this event at $B_x = 0$ at which usually E_y has been assigned the critical component.

2.3. Flow Event 2: August 8, 2019

Figure 3 displays MMS 1 data for fast flow event 2, which was measured at ∼17:15 UTC on August 8, 2019. The event was measured in the midnight sector close to the midnight meridian at $[-26.9, -0.7, 4.8]$ R_E (Figure 1). Figure 4a shows that MMS 1 measured mainly >2 keV ions in the plasma sheet. The energy flux at ∼10 keV intensified during the event.

V_x and $V_{\perp x}$ peak now at 400 km/s (Figures 4c and 4d). The magnetic field measurements show that B_z was fairly stable and positive during the event (Figure 4b). B_y was also positive with a somewhat higher and significant magnitude except at the trailing end of the fast flow. B_x showed a gradual reversal from positive to negative within a few minutes between 17:13 and 17:17 UTC over the flow event. IMF B_y was clearly positive varying around 3 nT (except a few short intervals during which it varied around zero) during more than four hours before the fast flow event (Figure 3c). This might explain the positive tail B_y values on the both sides of the neutral sheet around the flow event as well as for the several preceding hours (not shown). Long lasting clearly positive IMF B_y can have caused twisting of the closed field lines, which is seen in the prevailing positive tail B_y (Figure 4b). From the SME data, we see that the fast flow event was detected in the late recovery phase of a moderate substorm (SME maximum of 710 nT) (Figure 3d).

The B_x reversal was associated with a clear $V_{\perp y}$ reversal from dawnward to duskward right before 17:15:30 UTC in the middle of the fast flow (Figure 4c). The electric field data (Figures 4e–4g) indicate that the frozen-in condition holds during the flow event except at the early part of the event before 17:14:30 UTC, where the Z components of the two electric field estimates are found to deviate significantly (Figure 4g). E_y and E_z are generally positive and negative, respectively, during the event.

By comparing the terms constituting $V_{\perp y}$, we observe that $E_z B_x$ determines the dawn-dusk velocity component (Figure 4h). The magnitude of $-E_x B_z$ is very small and its contribution to the variations in $V_{\perp y}$ is insignificant. Therefore, also in this event, it is E_z and not E_x, which is the relevant electric field component in the determination of the dawn-dusk perpendicular velocity direction. The importance of E_z over E_y is also unambiguous in the $V_{\perp x}$ component (Figure 4i). The $E_y B_z$-term has only a negligible contribution to $V_{\perp x}$ compared with $-E_z B_y$. The event is thus another example of a fast flow where E_z is the more relevant electric field component compared with E_y and E_x.
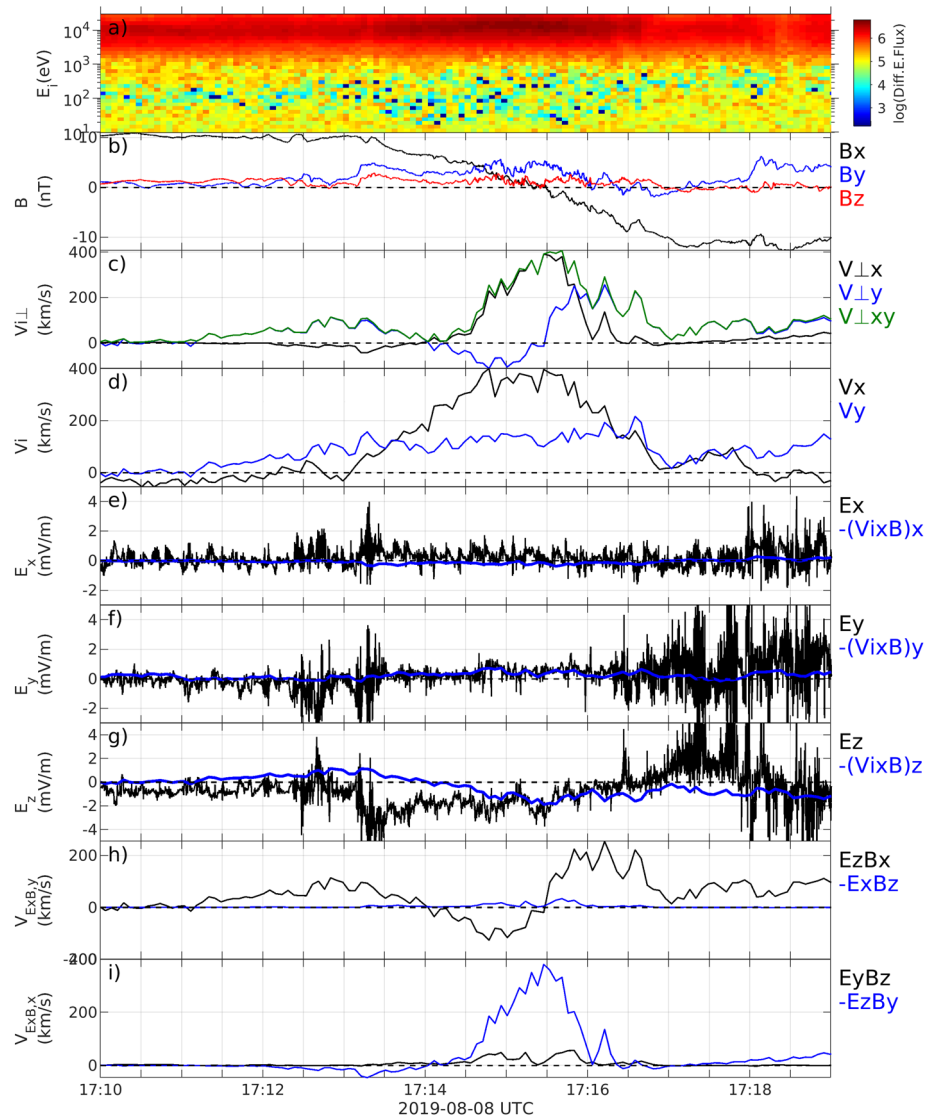
Figure 4. Same as Figure 2, but for flow event 2 on August 8, 2019.

2.4. Flow Event 3: July 12, 2017

The third fast flow event analyzed (flow event 3) was measured between ~15:34 and 15:39 UTC on July 12, 2017. Similar to event 2, this event was also measured in the midnight sector $[-24.4, 1.7, 5.3]$ R_E (Figure 1). Figure 5 displays the MMS 1 spacecraft data for the event. The differential energy flux data show that the spacecraft measured mainly >2 keV ions in the plasma sheet (Figure 5a).

In this event, V_x and $V_{\perp x}$ peak at almost 340 km/s (Figures 5d and 5c). The magnetic field shows that after a dipolarization front at 15:34:40 UTC, B_z stayed clearly positive over the duration of the flow event (Figure 5b). B_y was positive and quite strong (~5 nT). B_x instead had fluctuations between positive and negative values. The fact that B_y stayed clearly positive for both positive and negative B_x, suggests a possibility of field line twisting caused by the IMF. IMF B_y was generally weakly positive (<2 nT) for more than five hours preceding the flow event (Figure 3e). According to the SME data, the event was measured in the recovery phase of a weak substorm (SME maximum of 310 nT) (Figure 3f).

By comparing $V_{\perp y}$ (Figure 5c) to B_x (Figure 5b), it can be noted that the curves during the event are closely mirror images of each other. This indicates that, again, B_x is a contributing magnetic field component to the
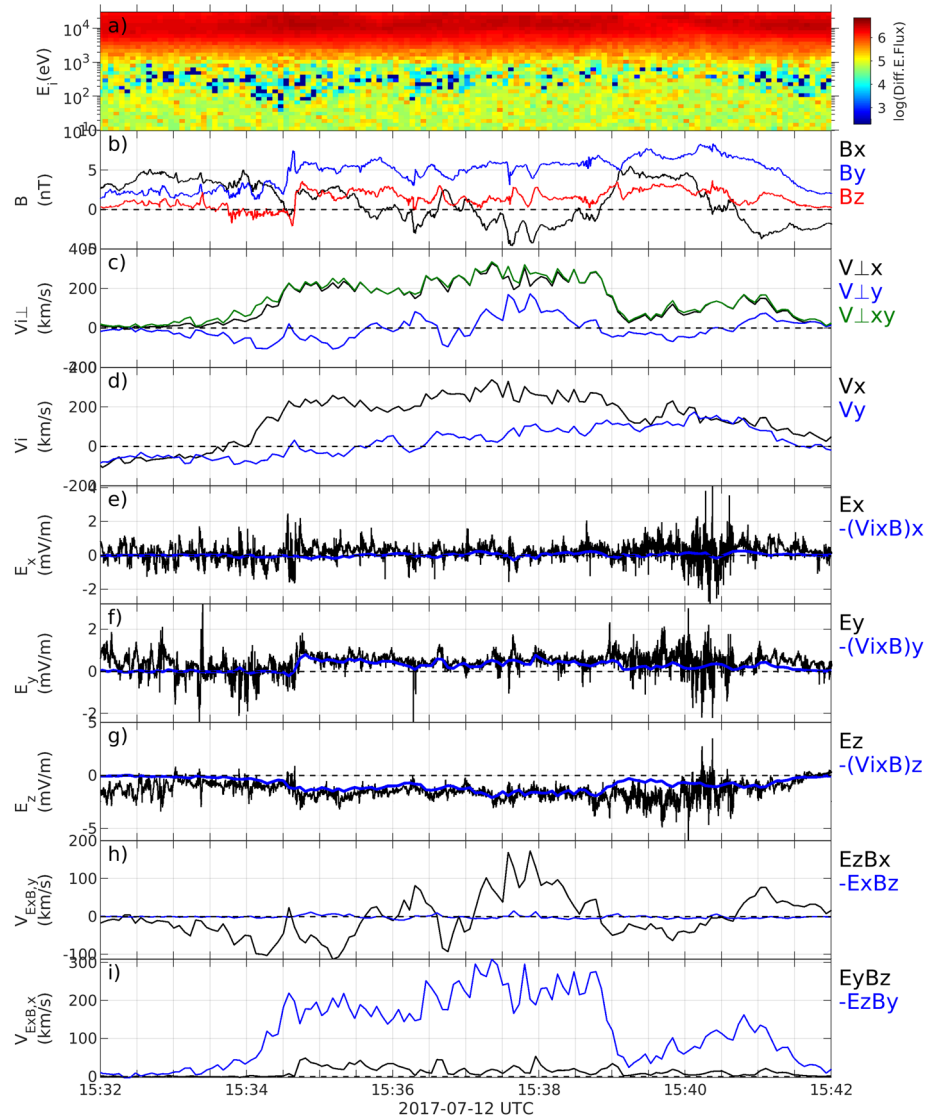
Figure 5. Same as Figure 2, but for flow event 3 on July 12, 2017.

perpendicular dawn-dusk velocity. From the electric field data, we can see that the frozen-in condition is satisfied during the event (Figures 5e–5g). E_y and E_z are positive and negative, respectively.

In Figure 5h, we observe that the E_zB_x-term determines $V_{\perp y}$. Similarly, in Figure 5i, the $-E_zB_y$ term determines $V_{\perp x}$. Thus, even in this fast flow event, E_z is the critical electric field component in determining $V_{\perp x}$ and $V_{\perp y}$, respectively.

2.5. Flow Event 4: August 4, 2017

The last fast flow event analyzed here, flow event 4, occurred at ~10:02 UTC on August 4, 2017. The event was measured in the premidnight sector at $[-21.5, 8.3, 2.6]$ R_E (Figure 1). The MMS 1 data for the event are displayed in Figure 6. The differential energy flux data for this event show that the spacecraft was in the plasma sheet measuring >2 keV ions during the event.

The highest values for V_x and $V_{\perp x}$ are ~740 and 560 km/s, respectively. Unlike the other fast flow events, this event lacks reversals in the magnetic field, except a short negative excursion in B_y at 10:02:34 UTC (Figure 6b). Otherwise, the magnetic field components were clearly positive during the event. Notably, B_z
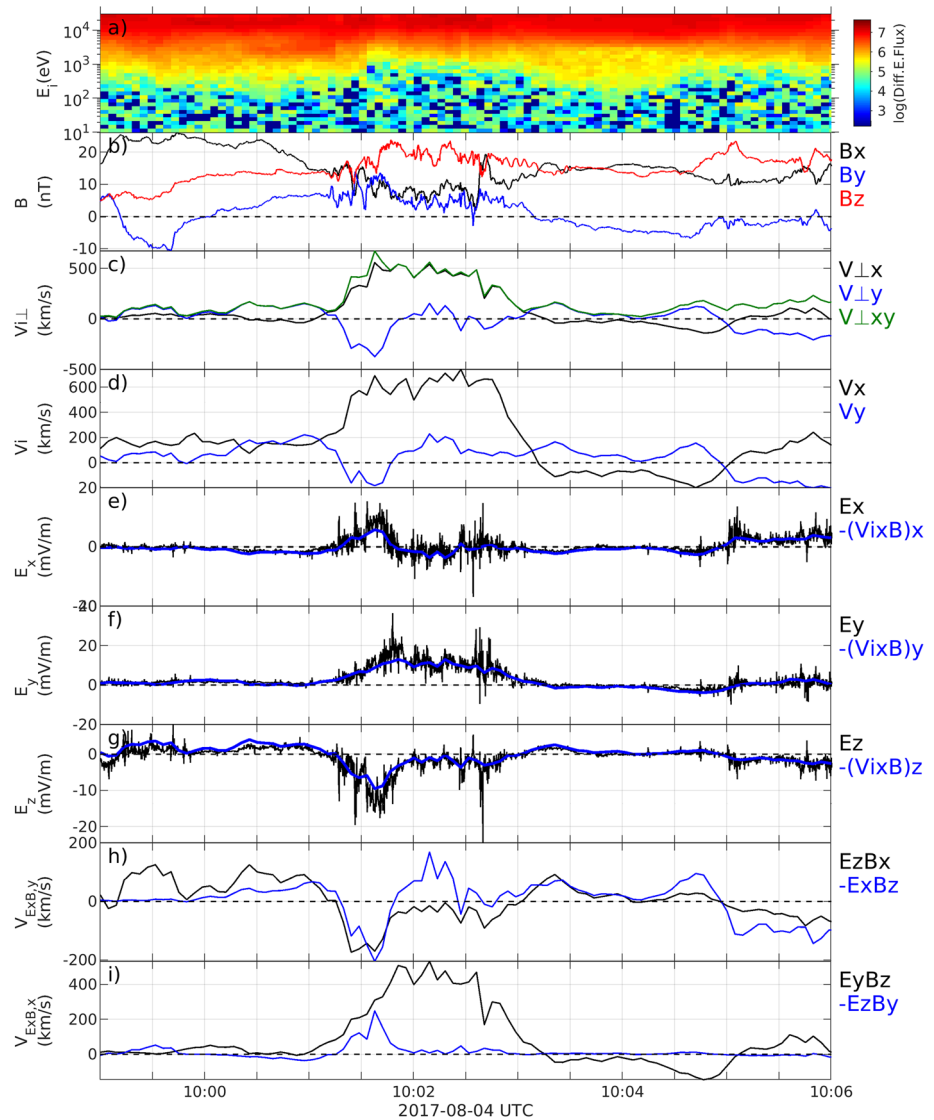
Figure 6. Same as Figure 2, but for flow event 4 on August 4, 2017.

appeared to be strong, ~20 nT and it exhibits a three-stage dipolarization front in the beginning of the fast flow. IMF B_y was strongly positive, being mostly between 10 and 18 nT during the preceding four hours (Figure 3g). This would imply the twisting of closed tail field lines. Some indication of this can be seen during the time intervals when the spacecraft resided closer to the neutral sheet, such as during the fast flow event. Tail B_y is directed duskward (twisted) while the flaring of the field lines in the premidnight sector would imply a dawnward direction for positive B_x. Note that the event was measured well in the premidnight sector in a region, where the influence of (positive) IMF B_y typically does not overcome the flaring effect and hence twist the tail magnetic field lines (Pitkänen et al., 2019). The SME data indicate that unlike the other events, this fast flow event was measured in the middle of strong substorm activity, the most intense electrojets (1,330 nT SME maximum) of which having already weakened though (Figure 3h).

When looking at the velocity data, it is noted that $V_{\perp y}$ reverses during the event (Figure 6c). Note that these occur now without the reversals in the magnetic field components. The reason must then be a varying electric field. The electric field data indeed show a variation in two components: E_x is significantly enhanced in the positive regime in the beginning of the fast flow and E_z in the negative regime (Figures 6e and 6g). E_y is stable and positive. The electric field data indicate that the frozen-in condition holds during the flow event.

The most interesting features appear in the comparison of the different terms for $V_{\perp y}$ and $V_{\perp x}$ (Figures 6h and 6i). In the beginning of the flow event, when dawnward $V_{\perp y}$ was measured, $E_z B_x$ and $-E_x B_z$ are comparable (Figure 6h). As E_x drops to small negative values (Figure 6e), the $-E_x B_z$-term intensifies and overcomes slightly negative $E_z B_x$ resulting duskward $V_{\perp y}$. In Figure 6i, we observe that except in the beginning of the fast flow, $E_y B_z$ solely determines $V_{\perp x}$. Thus, on the contrary to the previous flow events, in this event the E_x and E_y electric field components (and B_z) are relevant, not E_z, in the determination of the fast flow. The results are in line with the conventional view on fast flows.

3. Discussion

As discussed in Section 1, in the conventional picture, the dawn-to-dusk electric field component E_y together with the northward magnetic field component B_z are considered as the drivers of earthward convective fast flows in the magnetotail. We have demonstrated in the present study that the north-south electric field component E_z can play a dictating role not only in the determination of the dawn-dusk velocity ($V_{\perp y}$), but also in the determination of the enhanced earthward velocity ($V_{\perp x}$). This yields also near the neutral sheet in the presented fast flow events.

Huang and Frank (1994) have studied the average convection electric field in the tail plasma sheet using data from the ISEE-1 satellite in the tail range of $-23 < $ XGSM < 0 R_E. In their data set, Huang and Frank (1994) found that farther away from the neutral sheet (magnetic field magnitude $B > 25$ nT), the convection electric field has a major E_z component. In addition, in these conditions, E_z was found to be generally positive for $B_x > 0$ and negative for $B_x < 0$ in the premidnight sector. In the post-midnight sector, the E_z directions were found to reverse. Miyashita et al. (2020) have studied the average electric field in the plasma sheet in the tail range of $-32 < $ XGSM < -5 R_E using Geotail data. Their statistical results for E_z appear to be consistent with the results of Huang and Frank (1994) tailward of XGSM ~ -10 R_E, without limiting the magnitude of the magnetic field (Miyashita et al., 2020, their Figure 5). In the present study, generally all the four flow events occur with $B < 25$ nT and $E_z < 0$ irrespective of the B_x sign.

All our four fast flow events were associated with positive tail B_y. The magnitude of tail B_y was larger than the magnitude of tail B_z for the three events for which E_z was the most relevant electric field component. In the last flow event, where E_x and E_y were relevant, the magnitude of tail B_z was larger than that of tail B_y. It has been shown, that nonzero IMF B_y can have an influence on the tail magnetic configuration inducing an additional B_y component collinear to IMF B_y to the tail magnetic field, which leads to bending or twisting of the closed field lines (e.g., Kaymaz et al., 1994; Tenfjord et al., 2015). If IMF B_y in the events of the present study was affecting tail B_y in the plasma sheet causing twisting of the closed field lines, then the twisting is expected to be associated with a particular electric field. This is because the convection electric field is perpendicular to the magnetic field. In the case of positive tail B_y (and B_z), negative E_z for an earthward flow can be expected. Without the influence of IMF B_y and with no twist, small E_z magnitudes can be expected.

Pitkänen et al. (2018) have analyzed electric field data in an event, which has been interpreted as a twisted magnetotail (magnetic field) event (Pitkänen et al., 2016). Pitkänen et al. (2018) inferred that the E_z direction of the convection electric field on positively twisted field lines (positive tail B_y collinear to prevailing positive IMF B_y) should be southward, that is, $E_z < 0$, in line with the predictions by Nishida et al. (1998). In the flow events of the present study, we see that $E_z < 0$ generally in all the flow events, which is consistent with positive B_y and the results by Pitkänen et al. (2018).

The bending or twisting of magnetic field line directly affects the perpendicular flows, because these flows in the magnetotail (under the frozen-in condition) are generally determined by the $E \times B$ velocity. As noted in Section 1, previous event studies (Grocott et al., 2007; Pitkänen et al., 2015, 2018; Walsh et al., 2009) and statistical studies (Pitkänen et al., 2013, 2017, 2019) suggest an opposite $V_{\perp y}$ direction in both fast and slow perpendicular earthward flows above and below the neutral sheet ($B_x = 0$) if closed tail magnetic field lines are twisted. The results of the directions of $V_{\perp y}$ and B_x in the first three flow events shown in the present study are in accordance with these results. The last flow event 4 with a $V_{\perp y}$ reversal but with no B_x reversal does not fit fully to these previous results.

It is also possible that the tail B_y components associated with our flow events were not caused by the nonzero IMF B_y influence, but were originating from other effects. Petrukovich (2009) and Petrukovich (2011) have studied the contributions of different sources to tail B_y and point out that also the prevailing geomagnetic dipole tilt angle affects tail B_y. Specifically, Petrukovich (2011) found in Geotail data that for large tail B_y ($|B_y| > 5$ nT, and $|B_y| > $|IMF $B_y|$), the direction of large tail B_y statistically correlates with the sign of the dipole tilt angle and not with the IMF B_y direction in the near-Earth premidnight sector (XGSM $> -20\ R_E$, YGSM > 0). Our first flow event is within these constraints and we cannot rule out the dipole tilt angle effects influencing tail B_y. On the other hand, farther downtail (XGSM $< -20\ R_E$), large B_ys were found to be ordered mostly with IMF B_y of the same sign (Petrukovich, 2011). Our flow event 3 could be counted into this group. The formation of the large tail B_y configurations in the magnetotail is not yet understood, and the topic is beyond the scope of the present study.

Also notably, Case et al. (2020) found in a superposed epoch analysis, the unclear results for the response of the $V_{\perp y}$ direction above and below the neutral sheet in the midnight plasma sheet for reversals in the prevailing IMF B_y component. This analysis was covering time lags up to several hours from the reversals and the results indicate that we are still lacking understanding in what conditions are needed for an efficient IMF B_y influence on the magnetotail and its flows.

4. Summary

We have analyzed four earthward fast flow events measured by the MMS 1 spacecraft. The results demonstrate that the E_z electric field component can have a dictating role in the determination of the dawn-dusk perpendicular velocity. In addition, it is shown that the critical contribution of E_z is not limited only to $V_{\perp y}$, but it can also become dominant for the enhanced earthward flow component $V_{\perp x}$. The latter can occur also near and at the neutral sheet, which adds an alternative configuration to the conventional picture of E_y and B_z being mainly responsible in driving the earthward fast flows. The domination of E_z appears with potential signatures of an influence of a nonzero dawn-dusk component of the IMF B_y on the magnetotail.

We do not know how common are such fast flows where E_z is more relevant than E_y and E_x, where in the magnetotail they occur and in which solar wind and geomagnetic conditions. It is clear that these should be studied statistically. The increasing amount of MMS magnetotail measurements will make this possible. Such a statistical investigation is planned for a future study.

Data Availability Statement

The MMS data were accessed through the MMS Science Data Center, https://lasp.colorado.edu/mms/sdc/public/. The SuperMAG SME index data are available through https://supermag.jhuapl.edu.

References

Angelopoulos, V., Baumjohann, W., Kennel, C. F., Coronti, F. V., Kivelson, M. G., Pellat, R., et al. (1992). Bursty bulk flows in the inner central plasma sheet. *Journal of Geophysical Research*, *97*(A4), 4027–4039. https://doi.org/10.1029/91JA02701

Angelopoulos, V., Kennel, C. F., Coroniti, F. V., Pellat, R., Kivelson, M. G., Walker, R. J., et al. (1994). Statistical characteristics of bursty bulk flow events. *Journal of Geophysical Research*, *99*(A11), 21257–21280. https://doi.org/10.1029/94JA01263

Baumjohann, W., Paschmann, G., & Luehr, H. (1990). Characteristics of high-speed ion flows in the plasma sheet. *Journal of Geophysical Research*, *95*(A4), 3801–3809. https://doi.org/10.1029/JA095iA04p03801

Cao, J. B., Ma, Y. D., Parks, G., Reme, H., Dandouras, I., Nakamura, R., et al. (2006). Joint observations by Cluster satellites of bursty bulk flows in the magnetotail. *Journal of Geophysical Research*, *111*(A4), A04206. https://doi.org/10.1029/2005JA011322

Case, N. A., Grocott, A., Fear, R. C., Haaland, S., & Lane, J. H. (2020). Convection in the magnetosphere-ionosphere system: A multimission survey of its response to IMF By reversals. *Journal of Geophysical Research: Space Physics*, *125*(10), e27541. https://doi.org/10.1029/2019JA027541

Chen, C. X., & Wolf, R. A. (1993). Interpretation of high-speed flows in the plasma sheet. *Journal of Geophysical Research*, *98*(A12), 21409–21419. https://doi.org/10.1029/93JA02080

Ergun, R. E., Tucker, S., Westfall, J., Goodrich, K. A., Malaspina, D. M., Summers, D., et al. (2016). The axial double probe and fields signal processing for the MMS mission. *Space Science Reviews*, *199*(1–4), 167–188. https://doi.org/10.1007/s11214-014-0115-x

Gjerloev, J. W. (2012). The SuperMAG data processing technique. *Journal of Geophysical Research*, *117*(A9), A09213. https://doi.org/10.1029/2012JA017683

Grocott, A., Yeoman, T. K., Milan, S. E., Amm, O., Frey, H. U., Juusola, L., et al. (2007). Multi-scale observations of magnetotail flux transport during IMF-northward non-substorm intervals. *Annales Geophysicae*, *25*, 1709–1720. https://doi.org/10.5194/angeo-25-1709-2007

Huang, C. Y., & Frank, L. A. (1994). A statistical survey of the central plasma sheet. *Journal of Geophysical Research*, *99*(A1), 83–96. https://doi.org/10.1029/93JA01894

Kauristie, K., Sergeev, V. A., Kubyshkina, M., Pulkkinen, T. I., Angelopoulos, V., Phan, T., et al. (2000). Ionospheric current signatures of transient plasma sheet flows. *Journal of Geophysical Research*, *105*(A5), 10677–10690. https://doi.org/10.1029/1999JA900487

Kaymaz, Z., Siscoe, G. L., Luhmann, J. G., Lepping, R. P., & Russell, C. T. (1994). Interplanetary magnetic field control of magnetotail magnetic field geometry: IMP 8 observations. *Journal of Geophysical Research*, *99*, 11113–11126. https://doi.org/10.1029/94JA00300

King, J. H., & Papitashvili, N. E. (2005). Solar wind spatial scales in and comparisons of hourly Wind and ACE plasma and magnetic field data. *Journal of Geophysical Research*, *110*(A2), A02104. https://doi.org/10.1029/2004JA010649

Lindqvist, P. A., Olsson, G., Torbert, R. B., King, B., Granoff, M., Rau, D., et al. (2016). The Spin-plane double probe electric field instrument for MMS. *Space Science Reviews*, *199*(1–4), 137–165. https://doi.org/10.1007/s11214-014-0116-9

Miyashita, Y., Seki, K., Sakaguchi, K., Hiraki, Y., Nosé, M., Machida, S., et al. (2020). On the transition between the inner and outer plasma sheet in the Earth's magnetotail. *Journal of Geophysical Research: Space Physics*, *125*(4), e27561. https://doi.org/10.1029/2019JA027561

Nakamura, R., Baumjohann, W., Brittnacher, M., Sergeev, V. A., Kubyshkina, M., Mukai, T., & Liou, K. (2001). Flow bursts and auroral activations: Onset timing and foot point location. *Journal of Geophysical Research*, *106*(A6), 10777–10789. https://doi.org/10.1029/2000JA000249

Nakamura, R., Baumjohann, W., Schödel, R., Brittnacher, M., Sergeev, V. A., Kubyshkina, M., et al. (2001). Earthward flow bursts, auroral streamers, and small expansions. *Journal of Geophysical Research*, *106*(A6), 10791–10802. https://doi.org/10.1029/2000JA000306

Newell, P. T., & Gjerloev, J. W. (2011). Evaluation of SuperMAG auroral electrojet indices as indicators of substorms and auroral power. *Journal of Geophysical Research*, *116*(A12), A12211. https://doi.org/10.1029/2011JA016779

Nishida, A., Mukai, T., Yamamoto, T., Kokubun, S., & Maezawa, K. (1998). A unified model of the magnetotail convection in geomagnetically quiet and active times. *Journal of Geophysical Research*, *103*(A3), 4409–4418. https://doi.org/10.1029/97JA01617

Petrukovich, A. A. (2009). Dipole tilt effects in plasma sheet B_y: Statistical model and extreme values. *Annales Geophysicae*, *27*(3), 1343–1352. https://doi.org/10.5194/angeo-27-1343-2009

Petrukovich, A. A. (2011). Origins of plasma sheet B_y. *Journal of Geophysical Research*, *116*(A7), A07217. https://doi.org/10.1029/2010JA016386

Pitkänen, T., Hamrin, M., Karlsson, T., Nilsson, H., & Kullen, A. (2017). On IMF By-induced dawn-dusk asymmetries in earthward convective fast flows. In S. Haaland, A. Runov, & C. Forsyth (Eds.), *Dawn-dusk asymmetries in planetary plasma environments* (Vol. 230, pp. 95–106). American Geophysical Union.

Pitkänen, T., Hamrin, M., Kullen, A., Maggiolo, R., Karlsson, T., Nilsson, H., & Norqvist, P. (2016). Response of magnetotail twisting to variations in IMF B_y: A THEMIS case study 1-2 January 2009. *Geophysical Research Letters*, *43*, 7822–7830. https://doi.org/10.1002/2016GL070068

Pitkänen, T., Hamrin, M., Norqvist, P., Karlsson, T., & Nilsson, H. (2013). IMF dependence of the azimuthal direction of earthward magnetotail fast flows. *Geophysical Research Letters*, *40*, 5598–5604. https://doi.org/10.1002/2013GL058136

Pitkänen, T., Hamrin, M., Norqvist, P., Karlsson, T., Nilsson, H., Kullen, A., et al. (2015). Azimuthal velocity shear within an Earthward fast flow—Further evidence for magnetotail untwisting? *Annales Geophysicae*, *33*, 245–255. https://doi.org/10.5194/angeo-33-245-2015

Pitkänen, T., Kullen, A., Laundal, K. M., Tenfjord, P., Shi, Q. Q., Park, J. S., et al. (2019). IMF B_y influence on magnetospheric convection in Earth's magnetotail plasma sheet. *Geophysical Research Letters*, *46*(21), 11698–11708. https://doi.org/10.1029/2019GL084190

Pitkänen, T., Kullen, A., Shi, Q. Q., Hamrin, M., De Spiegeleer, A., & Nishimura, Y. (2018). Convection electric field and plasma convection in a twisted magnetotail: A THEMIS case study 1-2 January 2009. *Journal of Geophysical Research: Space Physics*, *123*, 7486–7497. https://doi.org/10.1029/2018JA025688

Pollock, C., Moore, T., Jacques, A., Burch, J., Gliese, U., Saito, Y., et al. (2016). Fast plasma investigation for magnetospheric multiscale. *Space Science Reviews*, *199*(1–4), 331–406. https://doi.org/10.1007/s11214-016-0245-4

Raj, A., Phan, T., Lin, R. P., & Angelopoulos, V. (2002). Wind survey of high-speed bulk flows and field-aligned beams in the near-Earth plasma sheet. *Journal of Geophysical Research*, *107*(A12). https://doi.org/10.1029/2001JA007547

Russell, C. T., Anderson, B. J., Baumjohann, W., Bromund, K. R., Dearborn, D., Fischer, D., et al. (2016). The magnetospheric multiscale magnetometers. *Space Science Reviews*, *199*(1–4), 189–256. https://doi.org/10.1007/s11214-014-0057-3

Schödel, R., Baumjohann, W., Nakamura, R., Sergeev, V. A., & Mukai, T. (2001). Rapid flux transport in the central plasma sheet. *Journal of Geophysical Research*, *106*(A1), 301–313. https://doi.org/10.1029/2000JA900139

Schödel, R., Nakamura, R., Baumjohann, W., & Mukai, T. (2001). Rapid flux transport and plasma sheet reconfiguration. *Journal of Geophysical Research*, *106*(A5), 8381–8390. https://doi.org/10.1029/2000JA900159

Sergeev, V. A., Sauvaud, J. A., Popescu, D., Kovrazhkin, R. A., Liou, K., Newell, P. T., et al. (2000). Multiple-spacecraft observation of a narrow transient plasma jet in the Earth's plasma sheet. *Geophysical Research Letters*, *27*(6), 851–854. https://doi.org/10.1029/1999GL010729

Shue, J. H., Ieda, A., Lui, A. T. Y., Parks, G. K., Mukai, T., & Ohtani, S. (2008). Two classes of earthward fast flows in the plasma sheet. *Journal of Geophysical Research*, *113*(A2), A02205. https://doi.org/10.1029/2007JA012456

Tenfjord, P., Østgaard, N., Snekvik, K., Laundal, K. M., Reistad, J. P., Haaland, S., & Milan, S. E. (2015). How the IMF B_y induces a B_y component in the closed magnetosphere and how it leads to asymmetric currents and convection patterns in the two hemispheres. *Journal of Geophysical Research: Space Physics*, *120*, 9368–9384. https://doi.org/10.1002/2015JA021579

Torbert, R. B., Russell, C. T., Magnes, W., Ergun, R. E., Lindqvist, P. A., Le Contel, O., et al. (2016). The FIELDS instrument suite on MMS: Scientific objectives, measurements, and data products. *Space Science Reviews*, *199*(1–4), 105–135. https://doi.org/10.1007/s11214-014-0109-8

Walsh, A. P., Fazakerley, A. N., Lahiff, A. D., Volwerk, M., Grocott, A., Dunlop, M. W., et al. (2009). Cluster and Double Star multipoint observations of a plasma bubble. *Annales Geophysicae*, *27*, 725–743. https://doi.org/10.5194/angeo-27-725-2009